

## Shaping T cell responses to factor VIII in hemophilia A with sialylated immunodominant peptides

by Eleonora Nardini, Sandrine Delignat, Brigitte-Carole Keumatio Doungstop, Katarzyna Olesek, Alejandra Reyes-Ruiz, Renaud Lavend'homme, Fabio Balzarini, Evert Peterse, Hakan Kalay, Rii-Jun E. Li, Ernesto Rodriguez, Sandra J. van Vliet, Marc Jacquemin, Sébastien Lacroix-Desmazes and Yvette van Kooyk

Received: September 29, 2025.

Accepted: June 17, 2026.

Citation: Eleonora Nardini, Sandrine Delignat, Brigitte-Carole Keumatio Doungstop, Katarzyna Olesek, Alejandra Reyes-Ruiz, Renaud Lavend'homme, Fabio Balzarini, Evert Peterse, Hakan Kalay, Rii-Jun E. Li, Ernesto Rodriguez, Sandra J. van Vliet, Marc Jacquemin, Sébastien Lacroix-Desmazes and Yvette van Kooyk. Shaping T cell responses to factor VIII in hemophilia A with sialylated immunodominant peptides. *Haematologica*. 2026 June 25. doi: 10.3324/haematol.2025.289279 [Epub ahead of print]

### *Publisher's Disclaimer.*

*E-publishing ahead of print is increasingly important for the rapid dissemination of science.*

*Haematologica is, therefore, E-publishing PDF files of an early version of manuscripts that have completed a regular peer review and have been accepted for publication.*

*E-publishing of this PDF file has been approved by the authors.*

*After having E-published Ahead of Print, manuscripts will then undergo technical and English editing, typesetting, proof correction and be presented for the authors' final approval, the final version of the manuscript will then appear in a regular issue of the journal.*

*All legal disclaimers that apply to the journal also pertain to this production process.*

# Shaping T cell responses to factor VIII in hemophilia A with sialylated immunodominant peptides

## Short title

SiaFVIII peptides control CD4+ responses in HA

## Authors

Eleonora Nardini<sup>1,2</sup>, Sandrine Delignat<sup>3</sup>, Brigitte-Carole Keumatio Doungstop<sup>1,2</sup>, Katarzyna Olesek<sup>1,2</sup>, Alejandra Reyes-Ruiz<sup>3</sup>, Renaud Lavend'homme<sup>4</sup>, Fabio Balzarini<sup>1,2</sup>, Evert Peterse<sup>1,5</sup>, Hakan Kalay<sup>1</sup>, Rui-Jún E. Li<sup>5</sup>, Ernesto Rodriguez<sup>1,2</sup>, Sandra J. van Vliet<sup>1,2</sup>, Marc Jacquemin<sup>4</sup>, Sébastien Lacroix-Desmazes<sup>3</sup> and Yvette van Kooyk<sup>1,2,5</sup>

## Authors affiliations

<sup>1</sup>Amsterdam UMC location Vrije Universiteit Amsterdam, Molecular Cell Biology and Immunology, Amsterdam, the Netherlands

<sup>2</sup>Amsterdam Institute for Immunology and Infectious diseases, Immunology, Amsterdam, the Netherlands

<sup>3</sup>Institut National de la Santé et de la Recherche Médicale, Centre de Recherche des Cordeliers, CNRS, Sorbonne Université, Université Paris Cité, Paris, France.

<sup>4</sup>Department of Cardiovascular Sciences, Center for Molecular and Vascular Biology, KU Leuven, Leuven, Belgium.

<sup>5</sup>AmbroSia, Amsterdam, The Netherlands

## Corresponding author

Yvette van Kooyk. E-mail: y.vankooyk@amsterdamumc.nl

## Acknowledgements

We thank Sara Garcia Garcia from the Microscopy and Cytometry Core Facility of Amsterdam UMC, and Helene Fohrer-Ting from the Cordeliers Research Centre for assisting in all flow cytometry experiments.

## Funding

This work was supported by the European Union's Horizon 2020 research and innovation program MSCA-ITN EDUC8 (859974) (E.N. and A.R.R) and MSCA-ITN-GLYTUNES (956758) (F.B.), FRM (FDT202304016725) (A.R.R), HEALTH HOLLAND (HH LSHM19073) (B.K.D.), NWO (SPI-93–538) (E.R.).

## Authors' disclosures:

The authors declare no competing financial or non-financial interests.

**Authors' contributions:**

Y.v.K., E.N. and S.D.L designed the research; E.N, S.D., K.O., B.C.K.D. performed research; E.P., H.K., M.J. and R.L. contributed vital reagents; E.N. analyzed data and made the figures; E.N. wrote the paper; all the others contributed to critically edit and review the paper.

**Data sharing statement:**

The data that support the findings of this study are available from the corresponding author upon reasonable request.

**Use of generative AI disclosure**

The authors declare that they used ChatGPT (OpenAI, GPT-4) to assist in language revision and refinement of the manuscript. All content was subsequently reviewed, verified, and edited by the authors.

Hemophilia A (HA) is a genetic disorder originating from a deficiency of coagulation factor VIII (FVIII). Up to 30% of severe HA patients develop neutralizing antibodies (inhibitors), which pose a serious threat to the success of replacement FVIII therapies. Immunologically, the development of inhibitors is a CD4-driven complication where T helper cells are key actors in inducing FVIII-specific memory B cells and plasma cells which secrete high levels of pathogenic IgGs<sup>1</sup>. Promising studies in HA preclinical models aiming at transiently depleting T cells showed an expansion of T<sub>regs</sub><sup>2</sup>, which are the counter-actors involved in maintaining tolerance towards FVIII in healthy individuals and likely restoring/promoting it in HA patients. A vast landscape of other tolerogenic solutions has been proposed, however, the immune response to FVIII in HA patients remains complex, warranting further studies to develop new tolerance-inducing strategies. A largely unexplored layer of complexity in the regulation of the immune response is glycosylation, the post-translational modification that adds glycans to proteins, lipids and RNAs to modify their function or signaling. In mammals, glycans are often capped by one specific monosaccharide, sialic acid. Sialylated glycans are recognized by immune cells via Siglecs, a family mainly comprising immune-inhibitory receptors. Engagement of Siglec-9 has already been explored as a treatment for allergies, showing induction of T<sub>regs</sub> *in vitro* and *in vivo* via modulation of dendritic cell (DC) function<sup>3,4</sup>. However, the way sialylation would modify the immune response to FVIII remains unclear as yet. In this study, we employed sialylated FVIII-derived (siaFVIII) peptides to investigate whether we could skew the anti-FVIII immune response towards tolerance. We demonstrate here with *in vitro* and *in vivo* experiments that siaFVIII-peptides can redirect CD4+ T cell responses by reducing activation, pro-inflammatory cytokine secretion and promoting T<sub>reg</sub> expansion.

FVIII has 4 glycosylation sites outside of the B domain, 3 of which are reported to be mostly sialylated<sup>5</sup>. Previous studies have linked a loss of sialic acids to increased inhibitor development<sup>6,7</sup>, suggesting a role for sialylation in regulating the immune response to FVIII. To examine how sialylation affects the immune response to FVIII, we chemically conjugated the C-terminal of various immunodominant peptides derived from FVIII to a sialylated glycan (siaFVIII-peptides, Figure 1A, Table 1). To meet experimental needs, different peptides were used throughout the study. Given that we both investigated human and mouse responses, we first used a 26 amino acid (FVIII1) peptide spanning a mouse and a human epitope. *In vivo*, a longer version, (FVIII1.1) of this peptide was employed, to account for correct antigen processing of the mouse epitope. The selection of this peptide sequence was guided by literature and by our previous study<sup>8</sup>, where we investigated *in silico* the promiscuity of binding to the most common HLA-DRB haplotypes and predicted > 75% worldwide population coverage. Moreover, to investigate the FVIII specific responses *in vitro*, a sequence specific for a CD4+ T cell clone was synthesized (FVIII2). All the sequences are within the C1 domain and the sialylated ones bind to Siglec-9 and its mouse homologue Siglec-E (Figure S1A, B).

We first investigated the ability of monocyte-derived DCs (moDCs) loaded with siaFVIII1 (sia-loaded moDCs) to instruct T cell responses (Figure 1B). Allogeneic co-cultures of CD4+ T cells with moDCs loaded with siaFVIII1 showed reduced

proliferation within the activated CD25+ subset compared to controls (Figure 1C), and this effect was partially dependent on Siglec-9, as suggested by knockout experiments (Figure S1C, D). This indicates that sia-loaded moDCs are less capable of initiating responses to non-FVIII allogeneic antigens, pointing to a broad, antigen-independent immunosuppressive effect mediated by siaFVIII1. Next, to investigate FVIII specificity, we employed a CD4+ T cell clone isolated from a HA patient (Figure 1D)<sup>9</sup>. Since this clone is specific for the epitope spanning amino acids 2113-2132, we used a longer peptide (FVIII2, Table 1) that includes this region to ensure proper antigen processing. HLA-DRB1\*01:01 / DRB1\*15:01 healthy donors were selected as source of moDCs, to match the genetic background of the T cell clone. Interestingly, we measured higher IFN- $\gamma$  concentrations in the supernatants from the T cell clone co-cultured with sia-loaded moDCs than control moDCs (Figure 1E). While IFN- $\gamma$  secretion from CD4+ T cells often signals a pathogenic Th1 response, in the context of a T cell clone it mainly reflects antigen presentation through MHC-II. Our results indicate that sialylation does not hinder, but rather enhances, MHC-II loading. By making use of a biotinylated version of FVIII2 and siaFVIII2, we measured binding / uptake in moDCs, showing that at 4°C siaFVIII2 binds better than FVIII2, partially dependently on Siglec-9 (Figure S1E). When the cells are put at 37°C and endocytosis is activated, siaFVIII2 and FVIII2 are equally taken up by moDCs (Figure S1F). Moreover, in the native FVIII protein, residue N2137 carries a mannosylated glycan, whose removal has been shown to reduce uptake by moDCs<sup>10</sup>, but synthetic peptides FVIII2 and siaFVIII2 lack this glycan. For these reasons, we postulate that the observed differences in antigen presentation are due to a receptor-mediated effect of sialylation on antigen processing, rather than altered peptide uptake by moDCs. We further observed that the T cell clone co-cultured with sia-loaded-moDCs expressed lower levels of CD69 and PD-1 than the control (Figure 1F, S1G,H). At such an early stimulation time point, this is indicative of reduced activation. Other cell surface markers were unaffected (Figure S1I, J). Our results suggest that moDCs process and present siaFVIII2 more efficiently than the unsialylated peptide to HA CD4+ T cell clones, while inducing a qualitatively different activation profile.

Then, we studied the immune response induced by siaFVIII-peptides in the preclinical model of HA (Figure 2A). The mice were treated with siaFVIII1.1 or the unsialylated peptide for 2 weeks prior of FVIII reconstitution, following a previously published dose-escalation protocol<sup>11</sup>, which is also an established method for immunotherapy in allergies. The development of anti-FVIII IgG was not affected by prophylactic treatment with siaFVIII1.1, but was increased in the unsialylated FVIII1.1-treated group, along with the inhibitor titers (Figure 2B). Accordingly, FVIII-specific splenic B cell populations were not altered upon pretreatment with siaFVIII1.1 (Figure S2A, B). Since FVIII1.1 is largely exposed on the surface of the C1 domain (Figure 2C), we measured anti-C1-peptide IgG, which correlated in our cohort with the inhibitor titers (Figure S2C). IgG towards FVIII1.1 and siaFVIII1.1 could be equally detected in both groups, but not in the PBS treated mice (Figure 2D), suggesting that the antibody response is directed against the peptide sequence, irrespective of the presence of the sialylated moiety. These results indicate that pretreatment with a single FVIII epitope selectively primed the immune response to that

sequence. Therefore, the PBS group was excluded from further analysis. Based on our *in vitro* results, we expected the T cell compartment to be modulated by siaFVIII pre-treatment. Remarkably, the analysis of the splenic T cell populations revealed higher percentages of T<sub>regs</sub> in the siaFVIII1.1-treated mice than in the unsialylated FVIII1.1-treated group (Figure 2E). Previous research already showed T<sub>regs</sub> induction with a model sialylated antigen<sup>12</sup>. Here, we show that a single sialylated FVIII immunodominant peptide can similarly modulate the immune response in the context of HA, maintaining the T<sub>regs</sub> compartment. T<sub>regs</sub> and conventional T cells (T<sub>convs</sub>) displayed distinct memory/effector phenotypes (Figure S2D), consistent with previous reports showing that naïve cells are more abundant among T<sub>convs</sub>, while T<sub>regs</sub> are enriched in central memory and effector subsets<sup>13</sup>. In our study, T<sub>regs</sub> phenotypes did not differ between the groups, whereas the siaFVIII1.1-treated group showed reduced frequencies of naïve and central memory T<sub>convs</sub> and increased effector cells (Figure S2E, F). We further tested *ex vivo* for the presence of peptide-specific T cells secreting IFN- $\gamma$  and TNF- $\alpha$ . Strikingly, the frequency of these cells in the siaFVIII1.1 group was reduced by half as compared to the unsialylated FVIII1.1-treated mice (Figure 2F). Previous research has shown that splenocytes from successfully tolerated mice restimulated with FVIII fail to secrete IFN- $\gamma$ <sup>14</sup>. Our findings *in vivo* imply that even though no differences in the humoral response were observed, the immune profile in the siaFVIII1.1 pre-treated mice may reflect a state of tolerance, characterized by suppression of T cells secreting IFN- $\gamma$  and TNF- $\alpha$ , while maintaining the T<sub>regs</sub> compartment. Concluding, this study demonstrates that sialylation of immunodominant peptides promotes a reduced-proinflammatory response to FVIII *in vitro* and modulates the CD4<sup>+</sup> T cell response *in vivo* by restraining T<sub>eff</sub> cells differentiation while preserving the T<sub>regs</sub> compartment. The shift in T cell fate towards T<sub>regs</sub>, together with previous studies assessing later time points in FVIII-tolerance<sup>6, 10, 11</sup>, suggest that a decline in inhibitor levels might occur over a longer follow-up period. Overall, these results suggest a novel approach to fine tune the immune system towards FVIII tolerance, laying the groundwork for future studies aimed at translating these immunological changes into clinical benefits.

### **Ethics statement**

The studies involving humans were approved by Medical Ethics Committee of Sanquin Blood Supply. The studies were conducted in accordance with the local legislation and institutional requirements. The participants provided their written informed consent to participate in this study. Animals were handled in agreement with local ethical authorities (APAFIS #44404-202308101204894 v5).

## References

1. Wroblewska A, Reipert BM, Pratt KP, Voorberg J. Dangerous liaisons: how the immune system deals with factor VIII. *J Thromb Haemost.* 2013;11(1):47-55.
2. Bertolini TB, Herzog RW, Kumar SRP, et al. Suppression of anti-drug antibody formation against coagulation factor VIII by oral delivery of anti-CD3 monoclonal antibody in hemophilia A mice. *Cell Immunol.* 2023;385:104675.
3. Hesse L, Feenstra R, Ambrosini M, et al. Subcutaneous immunotherapy using modified PhI p5a-derived peptides efficiently alleviates allergic asthma in mice. *Allergy.* 2019;74(12):2495-2498.
4. Keumatio Doungtsop BC, Nardini E, Kalay H, et al. Sialic acid-modified der p 2 allergen exerts immunomodulatory effects on human PBMCs. *J Allergy Clin Immunol Glob.* 2024;3(1):100193.
5. Qu J, Ma C, Xu X-Q, et al. Comparative glycosylation mapping of plasma-derived and recombinant human factor VIII. *PLoS One.* 2020;15(5):e0233576.
6. Vander Kooi A, Wang S, Fan MN, et al. Influence of N-glycosylation in the A and C domains on the immunogenicity of factor VIII. *Blood Adv.* 2022;6(14):4271-4282.
7. Ito J, Baldwin WH, Cox C, et al. Removal of single-site N-linked glycans on factor VIII alters binding of domain-specific monoclonal antibodies. *J Thromb Haemost.* 2022;20(3):574-588.
8. Nardini E, Keumatio Doungstop BC, Gerpe-Amor T, et al. Rational design of FVIII sialylated peptides to target Siglec-3 and Siglec-9 and improve peptide formulations for reverse vaccines. *Front Bioeng Biotechnol.* 2025;10:1558627.
9. Jacquemin M, Vantomme V, Buhot C, et al. CD4+ T-cell clones specific for wild-type factor VIII: a molecular mechanism responsible for a higher incidence of inhibitor formation in mild/moderate hemophilia A. *Blood.* 2003;101(4):1351-1358.
10. Delignat S, Rayes J, Dasgupta S, et al. Removal of mannose-ending glycan at Asn2118 abrogates FVIII presentation by human monocyte-derived dendritic cells. *Front Immunol.* 2020;11:393.
11. Pletinckx K, Nicolson KS, Streeter HB, et al. Antigen-specific immunotherapy with epitopes suppresses generation of FVIII inhibitor antibodies in HLA-transgenic mice. *Blood Adv.* 2022;6(7):2069-2080.

12. Perdicchio M, Ilarregui JM, Verstege MI, et al. Sialic acid-modified antigens impose tolerance via inhibition of T-cell proliferation and de novo induction of regulatory T cells. *Proc Natl Acad Sci U S A*. 2016;113(12):3329-3334.

13. Natalini A, Simonetti S, Favaretto G, et al. OMIP-079: Cell cycle of CD4(+) and CD8(+) naïve/memory T cell subsets, and of Treg cells from mouse spleen. *Cytometry A*. 2021;99(12):1171-1175.

14. Reipert BM, Sasgary M, Ahmad RU, Turecek PL, Schwarz HP. Blockade of CD40/CD40 ligand interactions prevents induction of factor VIII inhibitors in hemophilic mice but does not induce lasting immune tolerance. *Thromb Haemost*. 2001;86(6):1345-1352.

## Tables

ID	SEQUENCE	USE
FVIII1	K <sub>2155</sub> HNIFNPPIARYIRLHPTHYSIRST <sub>2180</sub>	In vitro moDC-T cell co cultures. In red is the mouse epitope, the human epitope is underlined.
FVIII2	A <sub>2108</sub> RQKFSSLYISQFIIMYSLDGKKWQTYRGNSTG <sub>2140</sub>	In vitro stimulation of the T cell clone. In red the epitope recognized by the T cells.
FVIII1.1	S <sub>2152</sub> GIKHNIFNPPIARYIRLHPTHYSIRSTLRM <sub>2183</sub>	<i>In vivo</i> prophylactic treatment of HA mice. In red is the mouse epitope, underlined the human epitope.
FVIII1.3	K <sub>2155</sub> HNIFNPPIARYIR <sub>2169</sub>	<i>Ex vivo</i> restimulation of the splenocytes.

Table 1. List of peptides used in the study. The full-length numbering for FVIII residues is used.

## Figure legends

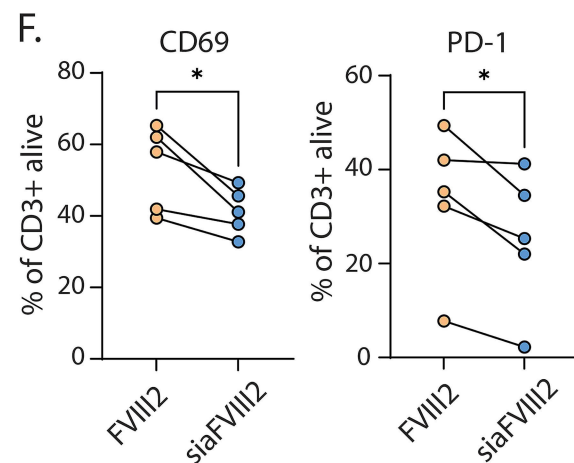
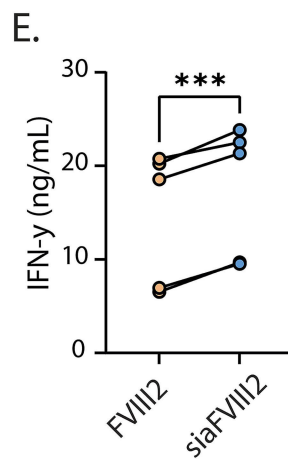
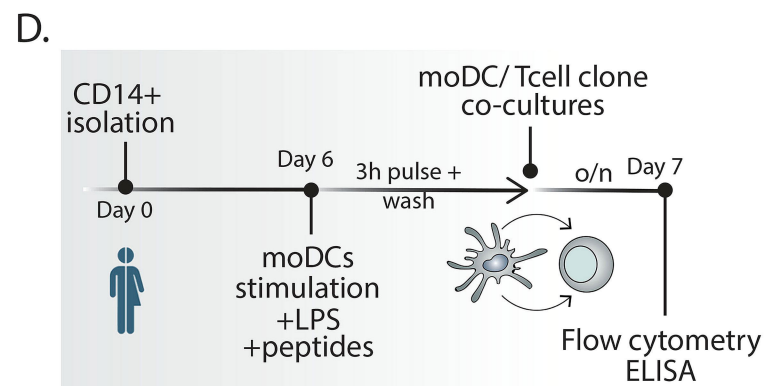
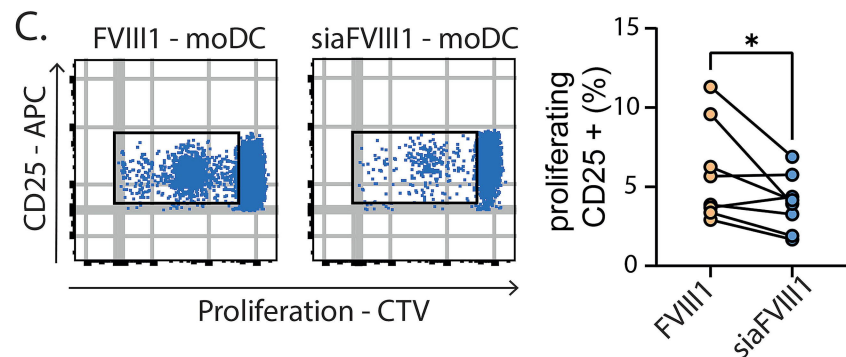
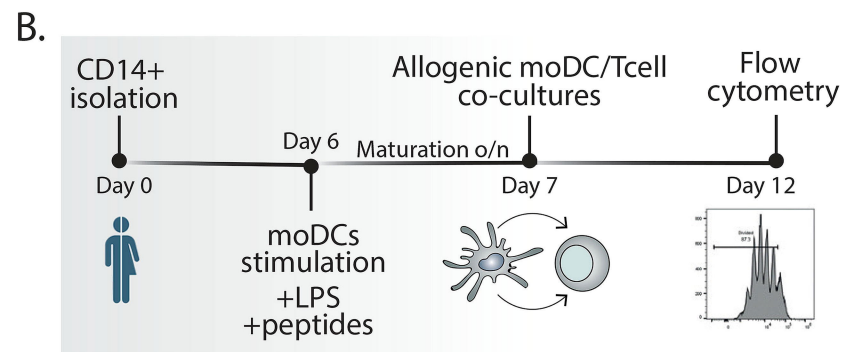
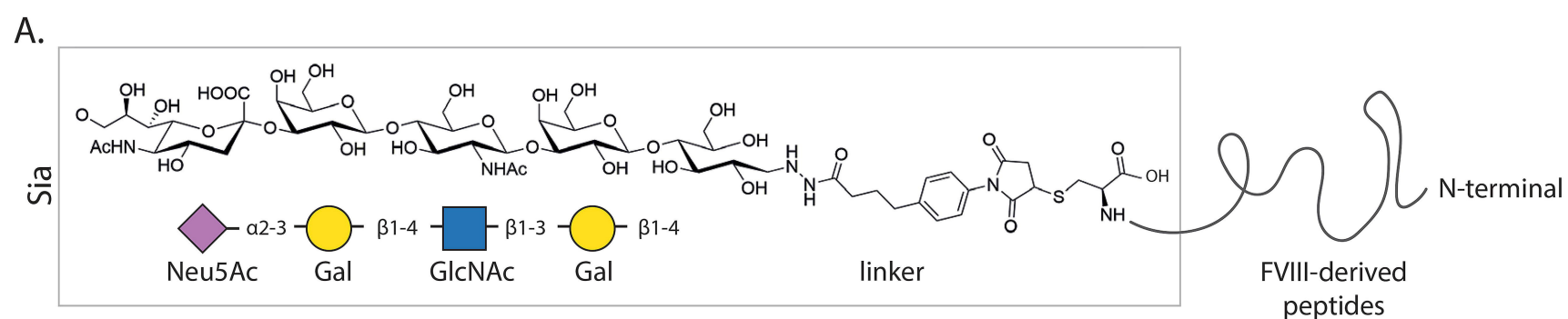
### Figure 1. moDCs loaded with siaFVIII-peptides dampen CD4+ T cell responses, both allogenic and HA-specific.

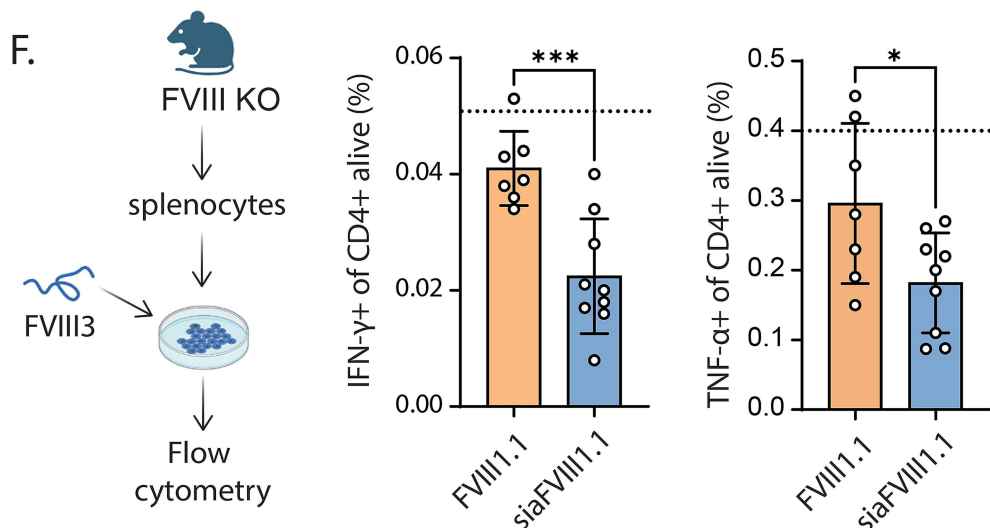
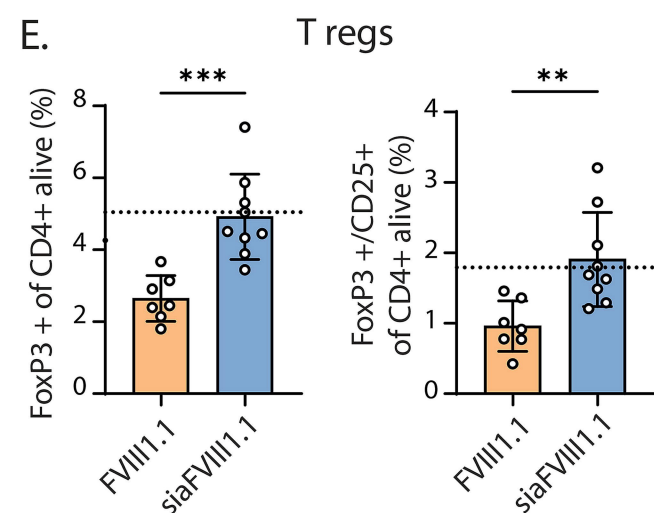
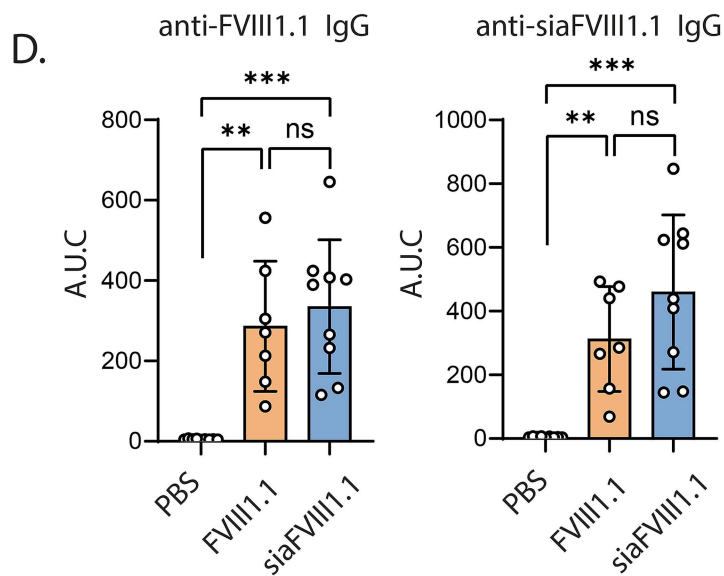
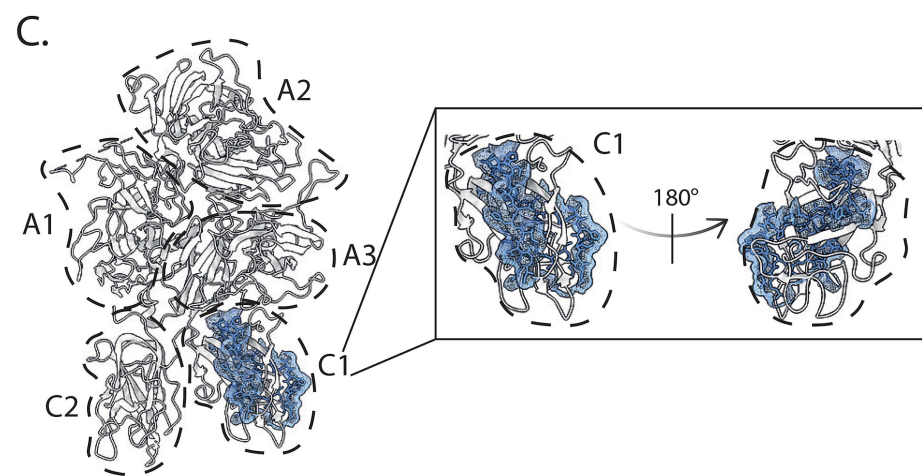
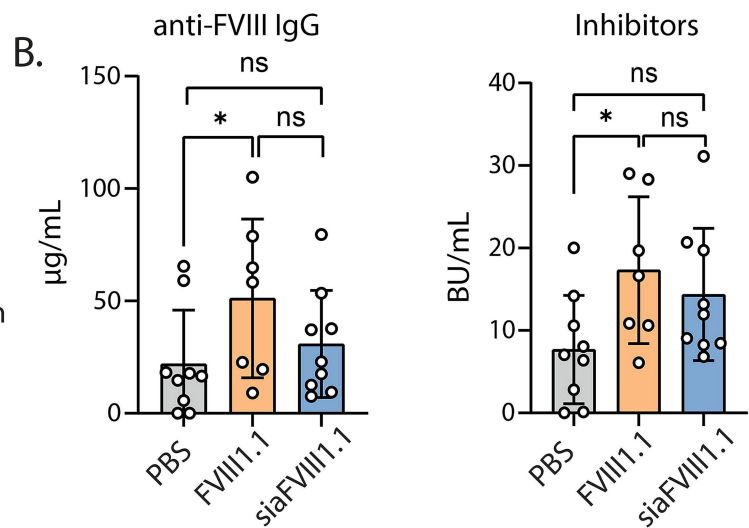
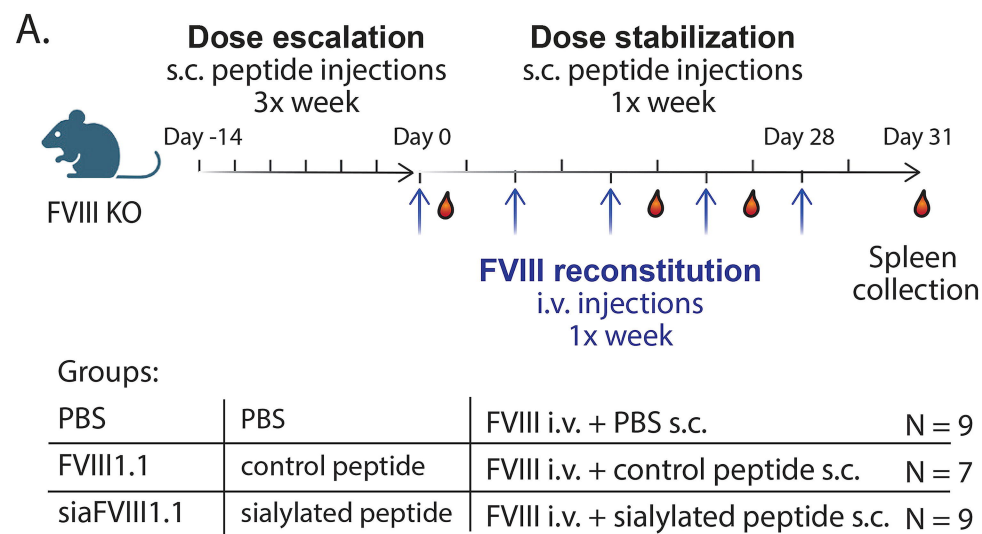
A. Schematic representation of the chemical structure of the tetrasaccharide and the linker coupled to the FVIII-derived peptides, obtained with ChemDraw. The tetrasaccharide is also shown following SNFG color-code. B. Schematic of the experimental workflow: moDCs obtained from CD14+ isolated monocytes from healthy donors were stimulated with FVIII1 or siaFVIII1 and matured overnight with 10 ng/mL of LPS. At day 7, co-cultures of moDCs : allogenic naïve CD4+ T cells (ratio 1 : 5) were established and kept in culture for 5 days to study T cell activation and proliferation. C. *left*, Representative dot plots showing the final gate of the gating strategy to select CD4+CD25+CTV- (proliferated) T cells. (not shown time, singlets, alive, CD4+); *right*, Quantification of proliferated T cells stimulated by FVIII1 (orange dots) or siaFVIII1 (blue dots)- loaded moDCs, shown as percentage of CD4+ alive. Each dot represents one moDC donor. N = 8. D. Schematic of the experimental workflow: moDCs obtained from CD14+ isolated monocytes from HLA-DRB1\*01:01/DRB1\*15:01 genotyped donors were stimulated with 0.5  $\mu$ M FVIII2 or siaFVIII2 for 3h in the presence of 10 ng/mL of LPS. Then, moDC : T cells (ratio 1 : 5) co-cultures with an HLA-matched CD4+ T cell clone isolated from an HA patient were established. The day after, the supernatants were collected to measure secreted IFN- $\gamma$  by ELISA and the cells were stained for flow cytometry analysis. E. Concentration of IFN- $\gamma$  in the supernatants of the T cell clone co-cultured with moDCs pulsed with 0.5  $\mu$ M of FVIII2 (orange dots) or siaFVIII2 (blue dots). Each dot represents the mean of 3 technical duplicates of one donor, N = 5. F. Percentages of CD69+ (*left*) and PD1+ (*right*) T cells from the T cell clone stimulated by FVIII2 (orange dots) or siaFVIII2 (blue dots)- loaded moDCs, measured by flow cytometry. N = 5 moDCs donors. Statistics: the data distribution was tested for normality by Kolmogorov-Smirnov test and parametric, paired t tests were computed accordingly. \* =  $p < 0.05$ , \*\*\* =  $p < 0.001$ .

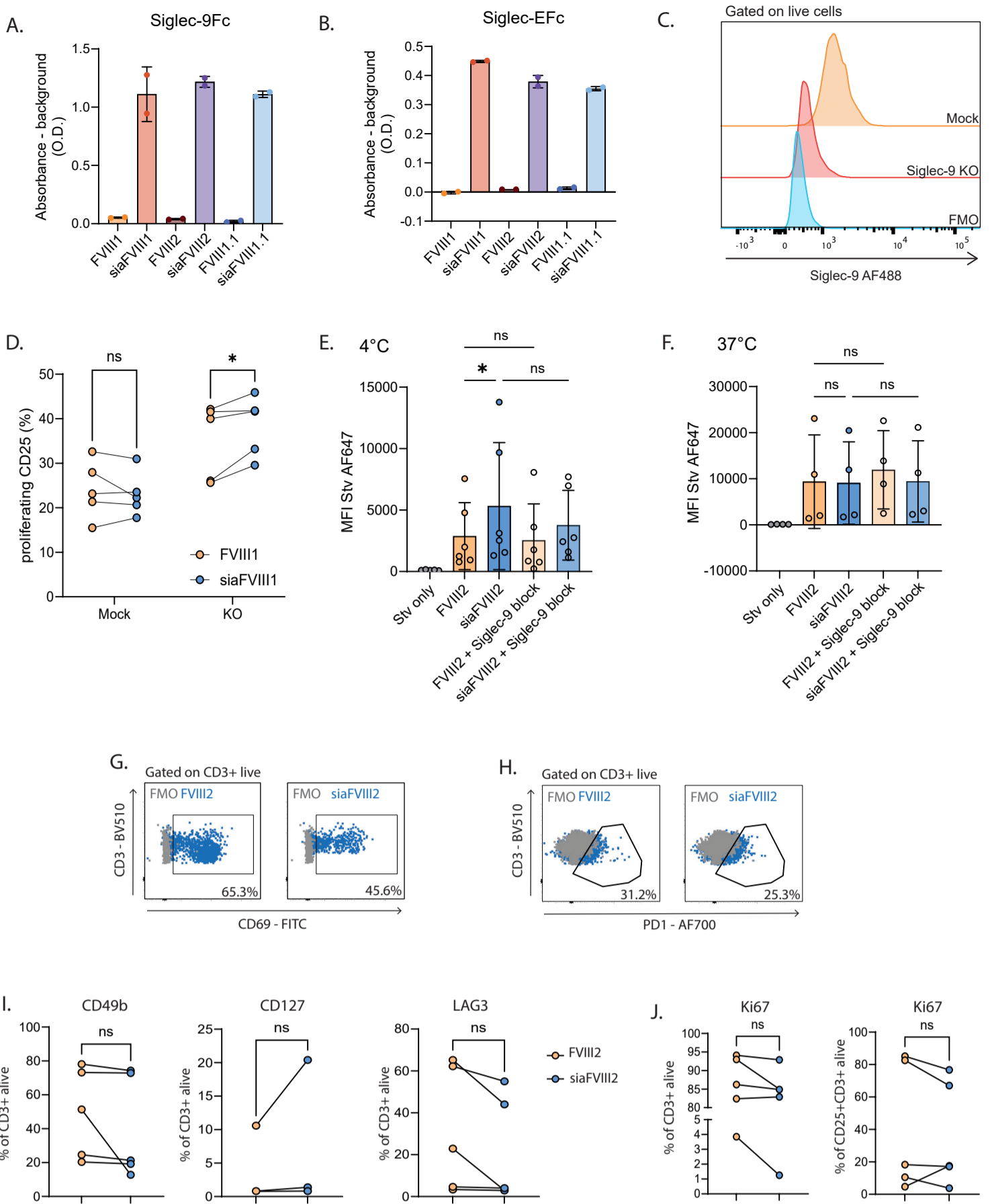
### Figure 2. Prophylactic treatment with siaFVIII-peptides significantly expands T<sub>regs</sub> and suppresses the activation of peptide-specific T cells.

A. Schematic of the immunization protocol. Groups of 7 or 9 FVIII-KO mice were treated 3 times per week for 2 weeks with s.c. injections in the neck of FVIII1.1 or siaFVIII1.1, or PBS according to a dose-escalation regimen (0.3 – 3 – 30 – 300 – 300 – 300  $\mu$ M of each peptide). After the peptide pretreatment, mice were immunized once per week for 5 weeks, via i.v. injections with 1 IU of full-length human FVIII. Subcutaneous treatment with FVIII1.1 or siaFVIII1.1, or PBS was continued s.c. once per week 3 days after every FVIII intravenous injection, following a dose stabilization regimen (300  $\mu$ M of each peptide). Blood samples were collected when indicated (red droplet). B. Titrations of anti-FVIII IgGs (*left*) and neutralizing anti-FVIII IgGs (*right*) in the sera samples collected at day 31 from mice pre-treated with PBS, FVIII1.1 or siaFVIII1.1, measured by ELISA and Bethesda Assay, respectively. Data are plotted as mean  $\pm$  standard deviation (SD). Each dot represents 1 mouse. Statistics: Kruskal-Wallis test with Dunn's post hoc correction for multiple comparisons. ns = non-significant, \* =  $p < 0.05$ . C. Three-dimensional structure of FVIII, the domains are indicated by a dotted line and FVIII1.1 is shown in blue in stick representation and dotted surface. The right panel shows a close-up view of the C1 domain with FVIII1.1. The model was

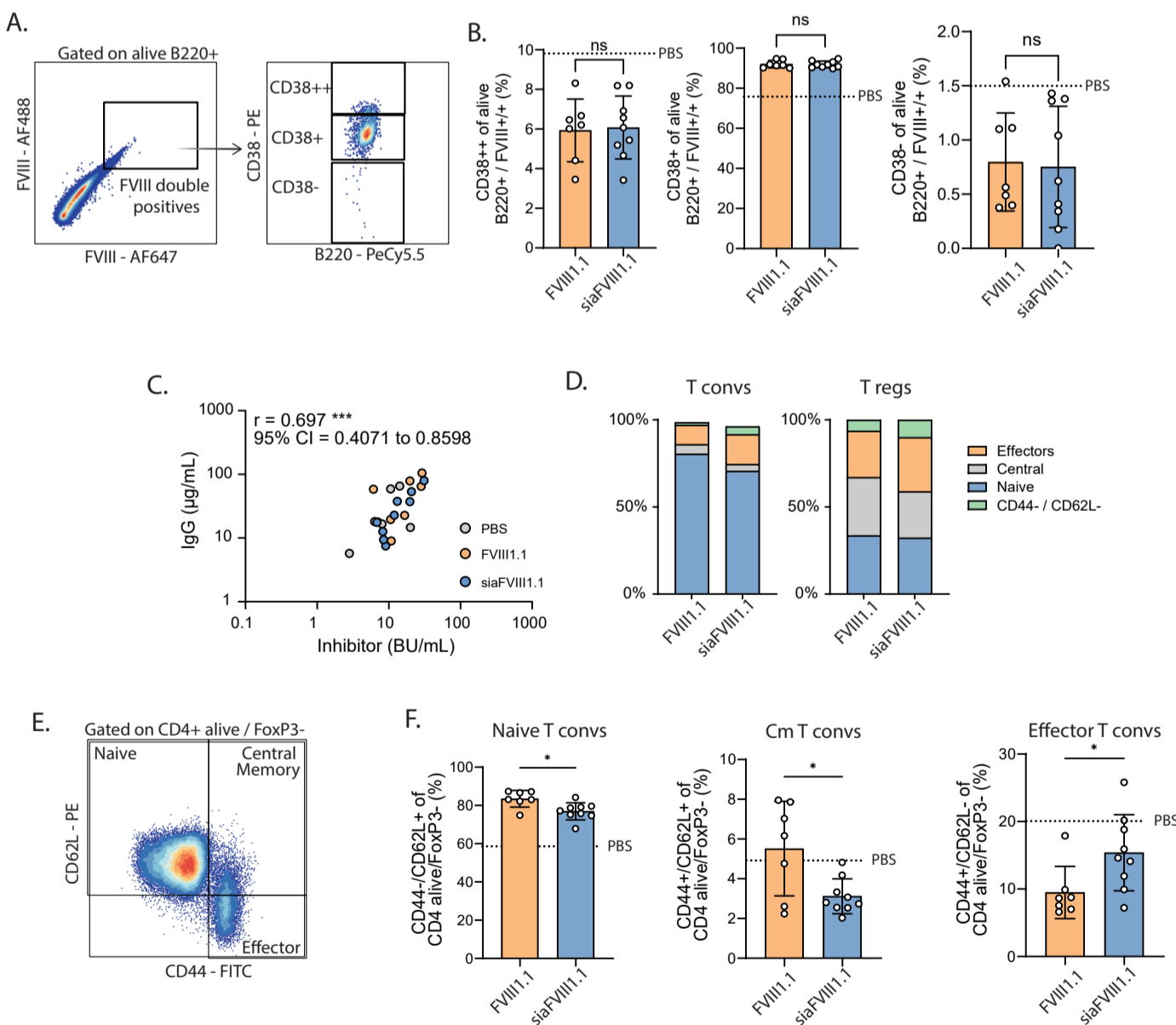
obtained with Chimera X software based on PDB file of FVIII 3CDZ. D. Quantification of anti- FVIII1.1 (*left*) and anti- siaFVIII1.1 (*right*) IgG in the sera samples collected at day 31 from mice pre-treated with PBS, FVIII1.1 or siaFVIII1.1. Maxi Sorp NUNC ELISA plates were coated with 2  $\mu$ M of FVIII1.1 (*left*) or siaFVIII1.1 (*right*) and incubated with serial dilutions of the sera. Anti-peptide IgG were detected with an anti-mouse-IgG-HRP and TMB substrate. The O.D. was plotted against the sera titration and the area under the curve (A.U.C.) was calculated. Data are plotted as mean  $\pm$  SD. Each dot represents 1 mouse. Statistics: Kruskal-Wallis test with Dunn's post hoc correction for multiple comparisons. ns = non-significant, \*\* =  $p < 0.01$ , \*\*\* =  $p < 0.001$ . E. Quantification of the percentages of FoxP3+ and FoxP3+/CD25+ T<sub>regs</sub> in the spleens. The dotted line represents the average of the PBS control mice. F. Schematic of the workflow for the *ex vivo* restimulation of the splenocytes and quantification of the percentages of IFN- $\gamma$  (*left*) and TNF- $\alpha$  (*right*) positive CD4+ T cells obtained from single cell suspensions of the spleens of mice pre-treated with FVIII1.1 or siaFVIII1.1. The cultures were restimulated *ex vivo* with the short peptide FVIII3, representing the CD4-restricted epitope included into the peptide FVIII1.1 used to immunize the mice. Cytokines are measured intracellularly by flow-cytometry. The dotted line represents the average of the PBS control mice. Data are plotted as mean  $\pm$  SD. Each dot represents 1 mouse. Statistics: the data distribution was tested for normality by Kolmogorov-Smirnov test and parametric or not-parametric unpaired t tests were computed accordingly. ns = non-significant, \* =  $p < 0.05$ , \*\* =  $p < 0.01$ , \*\*\* =  $p < 0.001$ .







**Supplementary Figure 1: A and B.** All the sialylated peptides used in the study bind to Siglec-9 and Siglec-E. The peptides were coated on a MaxiSorp ELISA plate at a concentration of 10  $\mu$ M and detected with 0.2  $\mu$ g/mL (Siglec-9Fc, A) or 2  $\mu$ g/mL (Siglec-EFc, B), and 0.2  $\mu$ g/mL of anti-IgG-HRP, visualized with TMB substrate. Data are presented as mean  $\pm$  SD. Each dot represents a technical duplicate. **C.** and **D.** Allogeneic co-cultures of CD4+ T cells with moDCs nucleofected with Cas-9 (mock) and loaded with siaFVIII1 showed reduced proliferation within the activated CD25+ subset compared to controls. On the other hand, moDCs nucleofected with Cas-9 pre-complexed with a gRNA targeting Siglec-9 (Siglec-9 KO) and loaded with siaFVIII1 induce higher proliferation of allogenic CD4+ T cells. C. Representative histogram showing Siglec-9 expression across moDCs mock and Siglec-9 KO. FMO is the fluorescence minus one control. D. Quantification of proliferated T cells stimulated by FVIII1 (orange dots) or siaFVIII1 (blue dots)- loaded moDCs, either mock or Siglec-9 KO. Each dot represents one moDC donor. N = 6. Statistics: paired t test. ns = not significant, \* =  $p < 0.05$ . **E.** and **F.** Biotinylated FVIII2 and siaFVIII2 are bound/internalized by moDCs. The binding/uptake was measured by pre-complexing the peptides with streptavidin-AF647 and incubating  $0.05 \times 10^6$  moDCs/well with 0.5  $\mu$ M of the peptides/streptavidin complexes for 1h at 4°C (E) or 37°C (F). Where indicated, the cells were pre-incubated with 10  $\mu$ g/mL of anti-Siglec-9 antibody. Data are presented as mean  $\pm$  SD. Each dot represents one donor and it is the average of two technical duplicates. Statistics: the data distribution was tested for normality by Kolmogorov-Smirnov test and Friedman test with Dunn's multiple comparisons correction was computed. \* =  $p < 0.05$ , ns = not significant. stv = streptavidin. **G** and **H.** Representative dot plots showing the final gate of the gating strategy to select live CD3+CD69+ (G.) and CD3+PD1+ (H.) cells. FMO = fluorescence minus one control. **I.** and **J.** Exhaustion markers and proliferation of the CD4+ T clone are not modified upon stimulation with moDCs loaded with FVIII2 or siaFVIII2. G. Percentages of CD49b, CD127, LAG3 positive T cell clones stimulated by FVIII2 (yellow dots) or siaFVIII2 (blue dots), measured by flow cytometry. N = 5 moDCs donors. H. Percentages of Ki67+ (left) and Ki67+/CD25+ (right) T cell clones stimulated by FVIII2 (yellow dots) or siaFVIII2 (blue dots), measured by flow cytometry. N = 5 moDCs donors. Statistics: the data distribution was tested for normality by Kolmogorov-Smirnov test and parametric or not-parametric paired t tests were computed accordingly. ns = not significant.



**Supplementary Figure 2. Prophylactic treatment with siaFVIII1.1 does not prevent the insurgence of FVIII-specific B cells.** **A.** Representative dot plots of the gating strategy used to identify FVIII double positive B cells by flow cytometry in the spleens of mice pre-treated with FVIII1.1 or siaFVIII1.1 or PBS. **B.** Percentages of CD38+, CD38+ and CD38- B cells in the spleens of mice pre-treated with FVIII1.1 or siaFVIII1.1, analyzed by flow cytometry. The mean of PBS group mice is indicated as a dotted line in each graph. **C.** Correlation between anti-FVIII IgG and inhibitors in sera collected at day 31 from animals treated with PBS (grey dots), FVIII1.1 (orange dots) or siaFVIII1.1 (blue dots). Statistics: Spearman correlation ( $r$ ); 95% confidence intervals (C.I.) are also shown. **D.** Stacked plots showing the distribution of naive, central, effector and double negative T cells in the T conventional (convs, left) and T reg (right) subsets measured by flow cytometry based on CD44/CD62L expression. **E.** Gating strategy to identify different conventional T cell subsets by flow cytometry in the spleens of mice pre-treated with FVIII1.1 or siaFVIII1.1 or PBS. **F.** Quantification of the percentages of naive, central memory (Cm) and effector T conventional (T convs) cells in the spleens of mice pre-treated with FVIII1.1 or siaFVIII1.1 or PBS analyzed by flow cytometry. The dotted line represents the means of mice pre-treated with PBS. Data are plotted as mean  $\pm$  standard deviation (SD). Each dot represents 1 mouse. Statistics: the data distribution was tested for normality by Kolmogorov-Smirnov test and parametric or not-parametric paired t tests were computed accordingly. ns = not significant, \* =  $p < 0.05$ .